

High bandwidth force estimation for optical tweezers

Hullas Sehgal, Tanuj Aggarwal, and Murti V. Salapaka

Department of Electrical and Computer Engineering, NanoDynamics Systems Laboratory,
University of Minnesota-Twin Cities, Minneapolis, Minnesota 55455, USA

(Received 23 September 2008; accepted 16 March 2009; published online 17 April 2009)

A prevalent mode of optical tweezers involves position clamping that regulates a constant position of a trapped bead. Traditional schemes employ the measured bead position in the open loop or the control signal in the position-clamp mode as an estimate of external force on the trapped bead. This article shows that traditional methods introduce fundamental limitations on bandwidth of the external force estimation. A method is presented that leads to an order of magnitude increase in the bandwidth of the external force estimation. Furthermore, a comprehensive modeling paradigm is introduced that facilitates estimation of forces on the bead. © 2009 American Institute of Physics. [DOI: 10.1063/1.3116621]

Dielectric particles when attached to single molecules provide a means for manipulating and interrogating molecules and thus provide *handles*¹ to the system of interest. In such studies, the information about the molecule is inferred by estimating² the force that tethered molecule exerts on the bead which is in an optical trap. Evidently, for such studies, estimating the force felt by the bead becomes the central objective of optical tweezer experiments.

Often the position of the bead is measured using a photodiode² that collects the laser that has passed through the bead. For the photodiode measurement to remain effective, the bead displacement has to be smaller than a few hundreds of nanometers.³ Thus feedback strategies become important, wherein based on the bead position measurement, a reference position close to zero is regulated to maintain measurement viability.³ Also, the regulating force F_r , applied on the bead becomes a measure of external forces acting on the bead.

In this article, it is shown that the regulating force does not provide an effective measure of the external force, if the external force being exerted has high frequency content. The main contribution of the article is a methodology, which overcomes limitations of using the regulating force as a measure of external forces, that is based on constructing and identifying a model of the dynamics that is capable of quantitatively matching the bead motion in real time.

The schematic of the experimental setup used is standard³ and is shown in Fig. 1, where a high power s -polarized component is used for trapping while the image of the trapped bead is projected onto the dual axis photodiode for detection using the low power p -polarized component that forms the reference beam. The regulating force on the bead is provided by changing the trap position using an acousto-optical deflector (AOD).

We now present preliminary material that will be used throughout the rest of the article. Consider an ordinary differential equation (ODE) in the variable z with input w ,

$$a_n \frac{d^n z}{dt^n} + a_{n-1} \frac{d^{n-1} z}{dt^{n-1}} + \cdots + a_0 z = b_m \frac{d^m w}{dt^m} + \cdots + b_0 w. \quad (1)$$

The *transfer function* $T(s)$ relating the Laplace transform, $w(s) := \int_0^\infty w(t)e^{-st}dt$, of the input $w(t)$ to the Laplace transform of the output $z(t)$ as $z(s) = T(s)w(s)$, where $T(s) = b_m s^m + \cdots + b_0 / a_n s^n + \cdots + a_0$. The stability of the ODE is gov-

erned by the roots of the characteristic polynomial of Eq. (1), i.e., the denominator of $T(s)$. The corresponding filter relating the Fourier transform $w(j\omega)$ of $w(t)$ to the Fourier transform $z(j\omega)$ of $z(t)$ is given by $z(j\omega) = T(j\omega)w(j\omega)$.⁴ Thus the filter $T(j\omega)$ represented by the ODE can be recovered from the transfer function. However, in the filter form $T(j\omega)$, the stability information of the ODE is not present.

Also, if $w(t)$ is a sinusoid $A \sin \omega t$ then the steady-state part of z that satisfies the ODE is $A|T(j\omega)|\sin(\omega t + \angle T(j\omega))$ and thus $T(j\omega)$ provides the scaling of the amplitude and the phase in the output z with respect to the input w . By the cutoff frequency of a filter will be meant the frequency $\omega/(2\pi)$, where $T(j\omega)/T(0)$ is -3 dB.

The equation of motion³ for the trapped bead for relatively small displacements⁵ is given by

$$\beta \dot{x} + k(x - u) = \eta(t) + F_e(t), \quad (2)$$

where x , u , k , η , and F_e are the instantaneous bead position, instantaneous trap position, trap's spring constant (in pN/nm), thermal noise force and the external force applied to the bead. Note that in Eq. (2) the bead position is controlled by using the AOD to move the trap position u that is equivalent to applying a force $F_r = ku$ on the bead. The photodiode measurement, y (in volts), of the bead position x varies linearly,³ in our setup, for $x < 500$ nm and the photodiode sensitivity S is 5 mV/nm. The transfer function representation for Eq. (2), with inputs F_e , $u=0$, and $\eta=0$ is $G(s) = 1/(\beta s + k)$ with cutoff frequency, $f_G = k/2\pi\beta$ Hz. Using the traditional power spec-

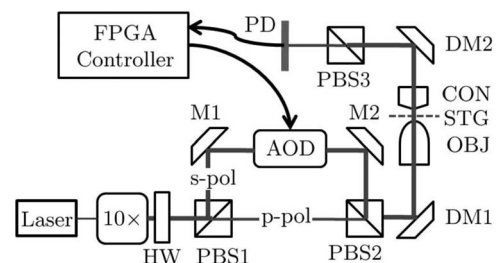


FIG. 1. Shows the optical tweezer experimental setup. Laser used is 500 mW, 1064 nm IR laser, 10× is the beam expander, HW is the half wave plate, PBS1, PBS2, and PBS3 are polarizing beam splitters, M1 and M2 are mirrors, DM1 and DM2 are dichroic mirrors. OBJ, STG, and CON are microscope objective, stage, and condenser, respectively. PD is the photodiode and FPGA controller contains the data acquisition and actuation logic.

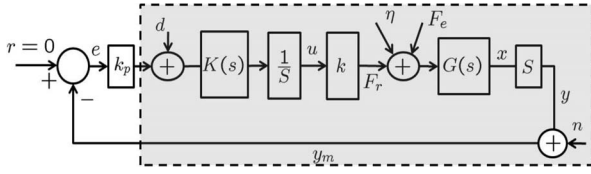


FIG. 2. Shows the closed-loop block diagram for the optical tweezer system with a proportional controller with a gain k_p . Inputs to the trapped bead, which is characterized by $G(s)$ are F_e , η , and F_r . The photodiode output y_m is compared with a constant reference signal, $r=0$, to maintain a constant bead position x . The transfer function $K(s)$ characterizes latencies present in the closed-loop implementation. The shaded part shows the block diagram for the identification of $P(s)=kK(s)G(s)$, where a frequency sweep input is applied as d and y_m is measured.

tral density method,⁶ k and β were determined to be $k=0.05$ pN/nm and $\beta=1.76 \times 10^{-5}$ pN s/nm.

In traditional open-loop schemes^{7,8} $u=0$ and the scaled photodiode output $F_o=ky_m/S$ is considered as an estimate of the force F_e . In this case

$$F_o(j\omega) = kG(j\omega)F_e(j\omega) = k \frac{1}{j\beta\omega + k} F_e(j\omega), \quad (3)$$

where F_o provides a good estimate^{7,8} of F_e if the Fourier transform of F_e is negligible beyond the cutoff frequency f_G .

In the position-clamp feedback setup (Fig. 2), the measured bead position is compared to a reference position r and based on the error, $e=r-y$, the controller provides a regulating force, $F_r=ku$. When a proportional gain controller⁵ with gain k_p is chosen, the closed-loop transfer function with input F_e and output F_r , in Fig. 2, is given by

$$F_r(s) = \frac{k_p P(s)}{1 + k_p P(s)} F_e(s), \quad (4)$$

where $P(s)=kG(s)K(s)$, where $K(s)$ captures latencies in the controller implementation. In existing work, it is assumed that the AOD instantly changes the trap position u once the command to change the trap position is given. Thus the existing feedback strategies (2) fail to capture the latencies [characterized by $K(s)$ in Fig. 2] and dynamics of components, like the AOD dynamics, that make them unsuitable for high bandwidth operation. A traditional closed-loop configuration² and analysis results from Fig. 2 if K is set to 1, where $F_{ra}=ku$ is considered as an estimate of the external force F_e . The closed-loop transfer function that relates F_e to F_{ra} (with K set to 1) is given by $F_{ra}(s)=\tilde{P}(s)/[1+\tilde{P}(s)]F_e(s)$, where $\tilde{P}(s)=kG(s)k_p$. Thus substituting for $G(j\omega)$ we have

$$F_{ra}(j\omega) = \frac{kk_p}{j\beta\omega + k(1+k_p)} F_e(j\omega). \quad (5)$$

The assumption that latencies represented by K can be ignored⁷ is reasonable if the external force F_e is such that $F_e(j\omega)$ is negligible beyond the cutoff frequency f_K of the filter $K(j\omega)$. In such a case, F_{ra} [see Eq. (5)] is a good approximation⁷ of F_r [see Eq. (4)] and Fourier components of F_e are accurately reconstructed up to the cutoff frequency, $f_{cla}=k(1+k_p)/2\pi\beta$ [see Eq. (5)]. The assumed closed-loop cutoff frequency $f_{cla}=f_G+kk_p/2\pi\beta$, thus the frequency up to which F_e can be correctly estimated by increases $kk_p/2\pi\beta$ over the open loop estimate. This advantage is limited as the controller gain k_p has to be small enough to maintain

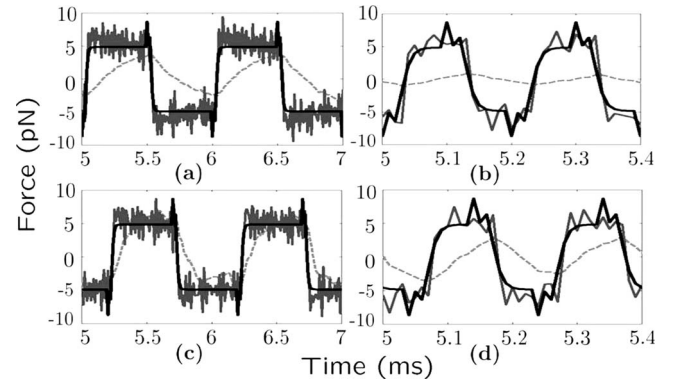


FIG. 3. Shows a comparison between the input force F_e (black solid line), the estimate of input force by the method developed in this paper, and the force estimate obtained using traditional methods. Plots (a) and (b) are for the open-loop case where 1 and 5 kHz periodic forces F_e are compared with \tilde{F}_o (gray solid line) and F_o (gray broken line). Plots (c) and (d) are for the closed-loop case where 1 and 5 kHz periodic forces F_e are compared with \tilde{F}_{cl} (gray solid line) and F_{ra} (gray broken line). The effect of thermal noise η was reduced from estimates by applying a Wiener filter.

stability³ of the closed loop and has to satisfy $f_{cla} < f_K$.

The limitations on the bandwidth of force estimation in both open and closed loop is evident in Fig. 3 that shows experimental data comparing F_e and the traditional estimates when F_e has high frequency content. F_e is a periodic wave of 1 kHz in Figs. 3(a) and 3(c) and 5 kHz in Figs. 3(b) and 3(d). Figures 3(a) and 3(b) show the open-loop estimates F_o and Figs. 3(c) and 3(d) show the traditional closed-loop estimates F_{ra} . It is evident that traditional estimates,^{7,8} F_o and F_{ra} , are not a good measure of the high bandwidth, more rapidly changing force profile. This forms the primary reason why low ATP (adenosine triphosphate) and salt concentrations are employed for motor protein studies² as low concentrations suppress the faster variations in the external force F_e and high frequency content in F_e due to higher concentration of ATP and salts under native conditions cannot be faithfully estimated by F_o and F_{ra} . We now introduce a modeling paradigm to overcome limitations of existing methods of estimating external forces that requires a better characterization methodology than employed by the existing methods.⁶

For accurately identifying the laser tweezer instrument dynamics (including the latencies K), the bead in the trap, without feedback, is subjected to a sinusoidal force $A \sin \omega t$ where A is chosen to reflect the maximum magnitude of the force that might be felt by the bead due to the external force under study (for the experiments in the paper, the parameter A was chosen to reflect typical force² magnitudes on the bead due to motor proteins). The sinusoidal force on the bead is exerted by moving the trap position using the AOD. The steady-state part of $y(t)$ will be of the form $|Y(j\omega)|\sin(\omega t + \phi_\omega)$ if the dynamics is linear and will have no other frequency component (other than at ω),⁴ where $|Y(j\omega)|$ denotes the magnitude by which the input sinusoid is amplified and ϕ_ω is the phase introduced by the dynamics. The absence of other frequency components in $y(t)$ confirmed linearity of the optical tweezer system for experiments in this article, with the frequency content at the output present primarily at the forcing frequency ω . The plot of $20 \log_{10}|Y(j\omega)|$ (dB) versus $\log_{10} \omega$ and ϕ_ω versus $\log_{10} \omega$ is shown in Fig. 4. Unlike the traditional power spectral density methods⁶ the frequency response (Fig. 4) of the system also provides the phase re-

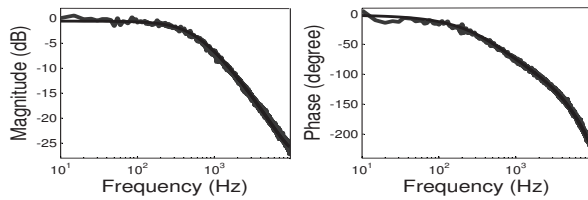


FIG. 4. Shows the frequency response of transfer function $P(s)$ obtained experimentally (in gray) and its estimate (in black).

sponse ϕ_ω and becomes crucial for identifying the latencies in the system that are not usually included in optical tweezers characterization.⁶ Given the frequency response data (Fig. 4), it is possible to obtain an ODE representation⁴ that relates the input d (in mV) to the output y (in mV). An ODE representation in the output y with an input forcing d was determined to be of the form $a_3 d^3 y/dt^3 + a_2 d^2 y/dt^2 + a_1 dy/dt + a_0 y = b_2 d^2 d/dt^2 + b_1 dd/dt + b_0 d$ that has a Laplace transform of the form

$$P(s) := \frac{Y(s)}{D(s)} = \frac{g_p(s - z_1)(s - z_2)}{(s + p_1)(s + p_2)(s + p_3)} \quad (6)$$

with $z_1 = 110$ krad/s, $z_2 = 97$ krad/s, $p_1 = 3$ krad/s, and $p_{2,3} = 41 \pm j43$ krad/s. The order of the ODE was chosen to match $P(j\omega)$ with the experimentally obtained frequency response (see Fig. 4) while keeping the order as small as possible. It follows from Fig. 2 that $P(s) = kK(s)G(s)$ which yields $K(s) = g_p(\beta s + k)(s - z_1)(s - z_2)/k(s + p_1)(s + p_2)(s + p_3)$ that has a cutoff frequency, $f_K = p_1/(2\pi)$ Hz. This completes identification of all components in Fig. 2.

The model obtained can be inverted to estimate the external force F_e over a larger frequency range. In the open-loop case, F_e passes through the filter $G(j\omega)$ to yield the output $x = y/S$ that is corrupted by measurement noise, n . Thus to obtain an estimate of F_e , $y_m/S = (y + n)/S$ can be filtered using the filter $G^{-1}(j\omega) = j\beta\omega + k$. Thus, open-loop estimate is provided by $G^{-1}(j\omega)(Y(j\omega) + N(j\omega))/S$. As G^{-1} is a high pass filter, it will unacceptably enhance the effect of noise. A better estimate can be obtained by introducing a stable low pass transfer function $Q(s) = 2\pi f_Q/(s + 2\pi f_Q)$, where f_Q is the cutoff frequency of Q , which is chosen based on the noise strength. y_m is filtered by $Q(j\omega)G^{-1}(j\omega)$ to yield a good estimate of F_e up to the cutoff frequency, f_Q , given by

$$\tilde{F}_o(j\omega) = Q(j\omega)F_e(j\omega) + Q(j\omega)G^{-1}(j\omega)N(j\omega)/S. \quad (7)$$

A similar method when employed for closed-loop case is more challenging. The transfer function that relates F_e to F_r (see Fig. 2) is $k_p P(s)/[1 + k_p P(s)] = k_p g_p(s - z_1)(s - z_2)/[(s + p_1)(s + p_2)(s + p_3) + k_p g_p(s - z_1)(s - z_2)]$, where z_1, z_2 are introduced into the dynamics due to system latencies. The inverse filter required to estimate the external force F_e from F_r is $[1 + k_p P(s)]/k_p P(s)$, which is unstable as it involves factors $(s - z_1)$ and $(s - z_2)$ in the denominator. This challenge can be overcome but will not be pursued here; however, we will use another readily available closed-loop signal y_m that circumvents this problem. The closed-loop filter that relates F_e to y_m/S is $G/(1 + k_p P)$ that has a stable inverse and can be implemented. Like in the open-loop case, a low pass filter $Q(s)$ is used to mitigate the measurement

noise. Thus a closed-loop estimate \tilde{F}_{cl} of F_e can be obtained by using the filter $Q(1 + k_p P)/G$ on y_m/S as provided below,

$$\tilde{F}_{cl}(s) = Q(s)F_e(s) + \frac{Q(s)[1 + k_p P(s)]N(s)}{G(s)S}, \quad (8)$$

that yields a good estimate up to the cutoff frequency f_Q .

It was illustrated earlier that the traditional strategies fail to reproduce good estimates of the external force F_e . Figures 3(a) and 3(b) also show the open-loop estimate \tilde{F}_o as obtained by the method developed in the paper (gray solid curve), where the 1 and 5 kHz periodic forces F_e are accurately predicted. The external force F_e experienced at the trapped bead has an amplitude of 5 pN (except in the region, where overshoots and undershoots are seen). It was confirmed that the force estimate obtained using the traditional method failed for a similar periodic profile of external force F_e at even 500 Hz (plot not shown). The experimental data confirm that using the method developed in this article, the temporal resolution of the external force estimation is improved by an order of magnitude in the open-loop case.

Figures 3(c) and 3(d) show the closed-loop estimate \tilde{F}_{cl} (gray solid line) obtained using Eq. (8) where the 1 and 5 kHz periodic forces F_e are accurately predicted. The input force F_e was generated by applying a square wave input d with 500 mV amplitude at 1 and 5 kHz. The cutoff frequency f_Q for the filter Q was chosen to be 100 kHz and k_p was set to 2. Figures 3(c) and 3(d) illustrate that the method developed in the paper is capable of estimating the periodic square wavelike force profile with a frequency of 5 kHz, whereas the traditional estimate fails at 1 kHz. The square wavelike periodic force has a significant contribution from second and third harmonics (which appear, respectively, at three and five times of the fundamental frequency), which implies that in the closed-loop case also, an order of magnitude increase in temporal resolution of force estimation is achieved by the method developed in the paper.

This paper highlights the deficiency of estimating high bandwidth input force as a reflection of the control input. An input force estimation scheme facilitated by the systems approach is applied to optical tweezer, enabling estimation of fast force dynamics and validated using experimental results. The improvement achieved in temporal resolution, sets the stage to investigate single molecule dynamics at higher ATP and salt concentrations.

This work was partly supported by NSF Grant Nos. CMMI0814615 and ECCS0814612 to Dr. Murti V. Salapaka.

¹S. M. Block, L. S. B. Goldstein, and B. J. Schnapp, *Nature (London)* **348**, 348 (1990).

²J. T. Finer, R. M. Simmons, and J. A. Spudich, *Nature (London)* **368**, 113 (1994).

³H. Sehgal, T. Aggarwal, and M. Salapaka, *Proc. SPIE* **2008**, 7038.

⁴A. V. Oppenheim and A. S. Willsky, *Signals and Systems*, 2nd ed. (Prentice Hall, Upper Saddle River, New Jersey, 1996).

⁵R. M. Simmons, J. T. Finer, S. Chu, and J. A. Spudich, *Biophys. J.* **70**, 1813 (1996).

⁶K. Visscher, S. Gross, and S. Block, *IEEE J. Sel. Top. Quantum Electron.* **2**, 1066 (1996).

⁷W. J. Greenleaf, M. T. Woodside, and S. M. Block, *Annu. Rev. Biophys. Biomol. Struct.* **36**, 171 (2007).

⁸M. Manosas, J. Wen, P. Li, S. Smith, C. Bustamante, I. Tinoco, and F. Ritort, *Biophys. J.* **92**, 3010 (2007).